Emission spectrum of a two-electron quantum dot molecule driven by a strong electromagnetic field

Andreas F. Terzis[1,2] and Emmanuel Paspalakis[3]
[1]*Department of Physics, School of Natural Sciences, University of Patras, Patras 26504, Greece*
[2]*Department of Physics, University of Cyprus, 1678 Nicosia, Cyprus*
[3]*Department of Materials Science, School of Natural Sciences, University of Patras, Patras 26504, Greece*
(Received 25 March 2009; published 13 July 2009)

We investigate analytically and numerically the emission spectrum of a two-electron quantum dot molecule in a continuous wave driving electromagnetic field. For high frequency driving our findings reveal that the analytic results based on a two-level approximate model predict correctly the emission spectrum for the low-frequency regime for any parameters values. The analytically predicted spectrum becomes of satisfactory agreement as we approach lower driving frequencies. Several features are reported from the numerical simulations, as harmonics splitting and high-harmonic generation, which cannot be explained in the context of the two-level scheme.

DOI: 10.1103/PhysRevB.80.035307 PACS number(s): 78.67.Hc, 42.65.Ky, 73.63.Kv, 42.50.Hz

I. INTRODUCTION

Double-coupled quantum dot (QD) structures, containing two electrons (usually referred to as a two-electron QD molecule), have received increasing interest recently.[1] This nanostructure is more complicated than a single-electron double QD structure as the strong Coulomb interaction between the two electrons should be included when the behavior of the system is studied. The interaction of the two-electron QD molecule with external electromagnetic fields has been the subject of several investigations, mainly dealing with the potential for controlled population dynamics and time-dependent wave functions of the system.[1–20]

Even though the dynamics of the two-electron QD molecule system is well studied, the photon emission spectrum of this system in the presence of an external oscillatory field has only been studied in one publication.[21] In Ref. 21 we presented results on the occurrence of high-order harmonic generation in a two-electron QD molecule under a low-frequency and high-intensity external electromagnetic field considering the coherent interaction of the QD structure with the field. We presented numerical calculations for a GaAs QD structure and compare our findings to results obtained from analytic expressions derived from a level-crossing model, with good agreement between analytical and numerical results.

We note that several articles have analyzed the emission spectrum of single-electron double-coupled QD structures interacting with high-frequency electromagnetic fields.[22–26] In addition, the photon emission spectrum of two-level quantum systems that are strongly driven by electromagnetic fields has been studied in several publications,[27–35] with emphasis given to the case of low-frequency driving fields and the occurrence of high-order harmonic generation.

In the present paper we study the emission spectrum of a two-electron QD molecule driven by an external oscillatory field. We consider the high-frequency driving-field regime so this study can be considered complimentary to our previous investigation.[21] Both numerical and analytical results are presented. For the low-frequency part of the spectrum the analytical results are in good agreement with the numerical results. However, this does not happen for the other regimes of the spectrum. Therefore, the validity of the analytical results is restricted. This is mainly because the analytical results are derived based on the assumption that the dynamics of the system can be well described by an effective two-level model. Also, the analytical expressions derived are rather complicated and take a simple form only in certain external frequency regimes.

II. QUANTUM SYSTEM, RELEVANT EQUATIONS AND ANALYTICAL RESULTS

The Hamiltonian of the two electrostatically interacting electrons in a QD molecule driven by an external electric field can be written as

$$H(t) = h(\vec{r}_1,\vec{p}_1,t) + h(\vec{r}_2,\vec{p}_2,t) + \frac{e^2}{\varepsilon|\vec{r}_1 - \vec{r}_2|}, \tag{1}$$

where $h(\vec{r},\vec{p},t)$ is the Hamiltonian of each electron. The third term expresses the Coulomb repulsion, where ε is the dielectric constant of the QD structure. The Hamiltonian $h(\vec{r},\vec{p},t)$ describing one electron confined in a double-dot structure is given by

$$h(\vec{r},\vec{p},t) = \frac{p^2}{2m} - ezE(t) + V_l(\vec{r}) + V_v(\vec{r}). \tag{2}$$

The first term describes the kinetic energy of the electron, with p being the momentum and m being the effective electron mass, the second term describes the interaction of the electron (in the dipole approximation) with an external field $E(t)$, and the last two terms represent the lateral and vertical confinement of the electron, respectively. The confinement potentials are described in harmonic-oscillator terms as[7,16]

$$V_l(\vec{r}) = V_l(x,y) = \frac{m\omega_z^2}{2}C(x^2 + y^2),$$

 ©2009 The American Physical Society

$$V_v(\vec{r}) = V_v(z) = \frac{m\omega_z^2}{8a^2}(z^2 - a^2)^2, \tag{3}$$

where ω_z is a characteristic angular frequency and C determines the strength of vertical confinement relative to the lateral confinement. In this representation the two QDs are centered at $\pm a$.

Our approach assumes that each QD contains only one energy level; the ground state of the one-electron system. This condition is achieved by proper selection of the lateral confinement, vertical confinement, and interdot distance.[7,16] From the one-particle wave vectors we generate six two-electron basis wave vectors, $\{|1,1\rangle, |1',1\rangle, |1,1'\rangle, |1',1'\rangle, |2,0\rangle, |0,2\rangle\}$, with respect to which we derive the matrix representation of the two-electron Hamiltonian. The left/right numerical index indicates the number of electrons in the left/right dot and the prime index distinguishes between spin-up and spin-down states. The two-particle basis can be rearranged so that it contains three spin-singlet and three spin-triplet states. The spin-triplet states with the electron number on each QD invariably one has no response to the applied electric field. Therefore, we ignore them and work with the reduced spin-singlet Hamiltonian, written using the spin-singlet basis $\{|2,0\rangle, [|1',1\rangle + |1,1'\rangle]/\sqrt{2}, |0,2\rangle\}$ as[7,9,16]

$$H(t) = \hbar \begin{bmatrix} V(t) & \sqrt{2}k & 0 \\ \sqrt{2}k & -W & \sqrt{2}k \\ 0 & \sqrt{2}k & -V(t) \end{bmatrix}. \tag{4}$$

Here, $W = W_1 - W_2$, with W_1 and W_2 being the intradot and the interdot Coulomb interaction of the electrons, k denotes the single-electron tunneling amplitude, and $V(t)$ describes the coupling between the electrons and the applied laser field.

The wave function of the QD system can be expanded in terms of the spin-singlet basis as

$$|\Psi(t)\rangle = a_1(t)|2,0\rangle + a_2(t)[|1',1\rangle + |1,1'\rangle]/\sqrt{2} + a_3(t)|0,2\rangle. \tag{5}$$

The dynamic evolution of the system is described by means of the time-dependent Schrödinger equation,

$$i\frac{d}{dt}\begin{bmatrix} a_1 \\ a_2 \\ a_3 \end{bmatrix} = \begin{bmatrix} V(t) & \sqrt{2}k & 0 \\ \sqrt{2}k & -W & \sqrt{2}k \\ 0 & \sqrt{2}k & -V(t) \end{bmatrix}\begin{bmatrix} a_1 \\ a_2 \\ a_3 \end{bmatrix}. \tag{6}$$

Once we know the temporal evolution of the probability amplitudes, the induced dipole can be calculated by the expression

$$\mu(t) = \tilde{\mu}[|a_1(t)|^2 - |a_3(t)|^2], \tag{7}$$

where $\tilde{\mu}$ is the electric dipole transition matrix element. The emission spectrum of the QD molecule can be estimated by means of the Fourier transform

$$S(\omega') = \left| \int e^{-i\omega' t}\mu(t)dt \right|^2. \tag{8}$$

Hence the coherent part of the emission spectrum of a typical two-electron QD molecule can be derived from the numerical solution of the time-dependent Schrödinger equation, Eq. (6). We concentrate on a typical GaAs QD structrure with parameters $\hbar\omega_z = 16$ meV, $C = 0.5$, and $a = 20$ nm leading to $\hbar W = 5.6$ meV and $\hbar k = -0.15$ meV.[7,9,11,16] Moreover, we take an ac electric field so $V(t) = \Omega\cos(\omega t)$, where Ω is the Rabi frequency describing the coupling of the QD structure with the external field and ω being the angular frequency of the applied field. The dynamic evolution of the system can also be described by a simpler set of equations, once the difference between the two types of Coulomb interaction W is much larger than $\sqrt{2}k$, as it is in the case studied here. Then,[9,11]

$$a_2(t) \approx \frac{\sqrt{2}k}{W}[a_1(t) + a_3(t)], \tag{9}$$

and the two-electron system is described by the following set of differential equations:

$$i\frac{d}{dt}\begin{bmatrix} a_1 \\ a_3 \end{bmatrix} = \begin{bmatrix} V(t) & \varepsilon \\ \varepsilon & -V(t) \end{bmatrix}\begin{bmatrix} a_1 \\ a_3 \end{bmatrix}, \tag{10}$$

where ε is defined as $\varepsilon \equiv \frac{2k^2}{W}$. It becomes obvious that the system reduces to an effective two-level system, where only the localized two-electron states are involved.

Obviously, Eq. (10) can be solved numerically as Eq. (6). However, here we make an effort to treat it analytically. The Hamiltonian of the two-level system can equivalently be written in terms of the well-known Pauli matrices σ_x, σ_z as

$$\begin{bmatrix} V(t) & \varepsilon \\ \varepsilon & -V(t) \end{bmatrix} = \begin{bmatrix} 0 & \varepsilon \\ \varepsilon & 0 \end{bmatrix} + \begin{bmatrix} V(t) & 0 \\ 0 & -V(t) \end{bmatrix} = \varepsilon\sigma_x + V(t)\sigma_z. \tag{11}$$

In the Heisenberg picture, the time-dependent induced dipole moment can be defined as

$$\mu(t) = \tilde{\mu}[a_1^*(0)\langle 2,0| + a_3^*(0)\langle 0,2|]\sigma_z(t)[a_1(0)|2,0\rangle + a_3(0)|0,2\rangle], \tag{12}$$

where

$$\sigma_z(t) = \begin{bmatrix} \sigma_z^{11}(t) & \sigma_z^{12}(t) \\ \sigma_z^{21}(t) & \sigma_z^{22}(t) \end{bmatrix} = \begin{bmatrix} \sigma_z^{11}(t) & \sigma_z^{12}(t) \\ [\sigma_z^{12}(t)]^* & -\sigma_z^{11}(t) \end{bmatrix}$$

is a time-dependent Pauli matrix, which becomes the ordinary Pauli matrix at $t = 0$,

$$\sigma_z(t=0) = \begin{bmatrix} 1 & 0 \\ 0 & -1 \end{bmatrix}.$$

In terms of the matrix elements of the $\sigma_z(t)$ matrix, the induced dipole becomes

$$\mu(t) = \tilde{\mu}[|a_1(0)|^2 - |a_3(0)|^2]\sigma_z^{11}(t) + \tilde{\mu}[a_1^*(0)a_3(0) + a_3^*(0)a_1(0)]\sigma_z^{12}(t). \quad (13)$$

From this expression it can be seen that the dipole moment of the QD molecule can be found once the temporal evolution of the Pauli matrix is known, for given initial conditions of the QD system.

Obviously, the time evolution of the dipole moment follows the dynamics of the components of the Pauli matrix. The temporal evolution of the Pauli matrices can be found from the Heisenberg equations of motion ($\frac{d\sigma_i}{dt} = \frac{i}{\hbar}[H, \sigma_i], i = x, y, z$) as

$$\frac{d}{dt}\begin{bmatrix}\sigma_+\\ \sigma_-\\ \sigma_z\end{bmatrix} = i\begin{bmatrix}2V(t) & 0 & -\varepsilon\\ 0 & -2V(t) & \varepsilon\\ -2\varepsilon & 2\varepsilon & 0\end{bmatrix}\begin{bmatrix}\sigma_+\\ \sigma_-\\ \sigma_z\end{bmatrix}, \quad (14)$$

where we have defined the $\sigma_\pm(t) = [\sigma_x(t) \pm i\sigma_y(t)]/2$ matrices.

By straightforward manipulation of these equations we can eliminate the $\sigma_\pm(t)$ matrices and find an expression for the derivative of the $\sigma_z(t)$ matrix that contains only the $\sigma_z(t)$ matrix. This is an integro-differential equation of the form[22–26]

$$\frac{d\sigma_z(t)}{dt} = -2i\varepsilon[\sigma_+(0)e^{i\Theta(t)} - \sigma_-(0)e^{-i\Theta(t)}] - 4\varepsilon^2\int_0^t dt'\sigma_z(t')\cos[\Theta(t) - \Theta(t')], \quad (15)$$

where $\Theta(t) = 2\int_0^t dt' V(t')$.

As $\sigma_+(t=0) = \left[\begin{smallmatrix}0 & 1\\ 0 & 0\end{smallmatrix}\right]$ and $\sigma_-(t=0) = \left[\begin{smallmatrix}0 & 0\\ 1 & 0\end{smallmatrix}\right]$, we find from Eq. (15) that

$$\frac{d\sigma_z^{11}(t)}{dt} = -4\varepsilon^2\int_0^t dt'\sigma_z^{11}(t')\cos[\Theta(t) - \Theta(t')], \quad (16a)$$

$$\frac{d\sigma_z^{12}(t)}{dt} = -2i\varepsilon e^{i\Theta(t)} - 4\varepsilon^2\int_0^t dt'\sigma_z^{12}(t)\cos[\Theta(t) - \Theta(t')]. \quad (16b)$$

By differentiating Eq. (13) and using Eqs. (16a) and (16b), we find the integrodifferential equation that the induced dipole moment of the QD molecule follows

$$\frac{d\mu(t)}{dt} = -2i\varepsilon\tilde{\mu}[a_1^*(0)a_3(0) + a_3^*(0)a_1(0)]e^{i\Theta(t)} - 4\varepsilon^2\int_0^t dt'\mu(t')\cos[\Theta(t) - \Theta(t')]. \quad (17)$$

We will now consider the tunneling initial condition where both the electrons are located in the same QD initially [$a_1(0) = 1$ or $a_3(0) = 1$]. As $\Theta(t) = 2\int_0^t dt' V(t') = (2\Omega/\omega)\sin(\omega t)$, then Eq. (17) reads

$$\frac{d\mu(\tau)}{d\tau} = -\tilde{\varepsilon}^2\int_0^\tau d\tau'\mu(\tau')\cos[\tilde{\Omega}\sin\tau - \tilde{\Omega}\sin\tau']. \quad (18)$$

Here, we defined the dimensionless parameters $\tau = \omega t$, $\tilde{\Omega} = 2\Omega/\omega$, and $\tilde{\varepsilon} = 2\varepsilon/\omega$. Applying the well-known Jacobi-Anger identities,[36]

$$\cos(z\sin\theta) = J_0(z) + 2\sum_{n=1}^{\infty} J_{2n}(z)\cos(2n\theta)$$

and

$$\sin(z\sin\theta) = 2\sum_{n=1}^{\infty} J_{2n-1}(z)\sin((2n-1)\theta),$$

Eq. (18) can be rewritten as

$$\frac{d\mu(\tau)}{d\tau} = -[\tilde{\varepsilon}J_0(\tilde{\Omega})]^2\int_0^\tau d\tau'\mu(\tau') - \tilde{\varepsilon}^2 G(\mu;\tau'), \quad (19a)$$

with

$$G(\mu;\tau') = 2\sum_{n=1}^{\infty} J_{2n}(\tilde{\Omega})\cos(2n\tau)\int_0^\tau d\tau'\mu(\tau') \times\left[J_0(\tilde{\Omega}) + 2\sum_{m=1}^{\infty} J_{2m}(\tilde{\Omega})\cos(2n\tau')\right] + 2\sum_{n=1}^{\infty} J_{2n+1}(\tilde{\Omega})\cos[(2n+1)\tau]\int_0^\tau d\tau'\mu(\tau') \times\left[2\sum_{m=0}^{\infty} J_{2m+1}(\tilde{\Omega})\cos(2n\tau')\right]. \quad (19b)$$

One can give a formal solution to Eq. (19a) as

$$\mu(\tau) = \tilde{\mu}\cos(\tilde{\varepsilon}J_0(\tilde{\Omega})\tau) - \tilde{\varepsilon}^2\int_0^\tau d\tau' \times\cos[\tilde{\varepsilon}J_0(\tilde{\Omega})(\tau - \tau')]G(\mu;\tau'). \quad (20)$$

In the case of a high-frequency driving field where $\omega \gg 2\varepsilon$ (i.e., $\tilde{\varepsilon} = 2\varepsilon/\omega \ll 1$), the solution of Eq. (20) can be considered by perturbation expansion with respect to the parameter $\tilde{\varepsilon}$.

III. NUMERICAL RESULTS AND DISCUSSION

We begin the discussion for very high-frequency driving fields. In this case, in the zero-order approximation the dominant term is the first term of Eq. (20). The dipole moment is simply $\mu(\tau) = \tilde{\mu}\cos[\tilde{\varepsilon}J_0(\tilde{\Omega})\omega t]$ and its Fourier transform [see Eq. (8)] has a peak at frequency $\tilde{\varepsilon}J_0(\tilde{\Omega})\omega$. As $\tilde{\varepsilon} \ll 1$ and $J_0(\tilde{\Omega}) \leq 1$ (for any value of the Rabi frequency), this peak corresponds to low-frequency generation [$\omega_{\mathrm{LF}} = \tilde{\varepsilon}J_0(\tilde{\Omega})\omega$]. However, the intensity of this low-frequency peak is expected to be very high since $\tilde{\mu}$ is the highest amplitude a Fourier component can have. Moreover, if the field intensity

and the driving frequency have a relation such that $J_0(\tilde{\Omega})=0$, i.e., $\tilde{\Omega}$ is a root of the zero-order Bessel function, the low-frequency peak tends to zero and the induced dipole moment gets a static value. This is a direct evidence of the two-electron localization condition[1,3,5–14,16] in the emission spectrum.

We have compared the results predicted by the analytic expression for the low frequency, ω_{LF}, with the predictions of the Fourier transform of the dipole moment derived by the numerical solution of the time-dependent Schrödinger equation [Eq. (6)]. We remind that the numerical solutions are valid in any regime and not only for the high-frequency driving regime. Our investigation reveals that there is an excellent agreement between the numerical and analytical results on the low-frequency generation, for cases not only with $\tilde{\varepsilon} \ll 1$ (high-frequency driving) but also up to $\tilde{\varepsilon} \approx 1$. This upper limit of $\tilde{\varepsilon}$ corresponds to frequency of the field photons equal to the splitting between the energy states in the effective two-level system. We stress that the frequency $\tilde{\varepsilon} J_0(\tilde{\Omega})\omega$ is present in any emission spectrum, even for very low-frequency driving fields. But for low-frequency driving fields, $\tilde{\varepsilon} J_0(\tilde{\Omega})\omega$ does not correspond to the lowest frequency of the spectrum and we find even lower frequencies, which can be explained from the two-level model analysis as contributions from the second term of Eq. (20), as now $\tilde{\varepsilon}$ is not small. In this regime of the driving-field frequency, it is quite reasonable to find harmonics below $\tilde{\varepsilon} J_0(\tilde{\Omega})\omega$, as this frequency can be quite high, especially for weak applied field. In the case of weak fields the Rabi frequency is close to zero and the zero-order Bessel function has a value close to unity $[J_0(0) \approx 1]$. Then the frequency $\tilde{\varepsilon} J_0(\tilde{\Omega})\omega$ of the emission spectrum depends practically solely on the value of $\tilde{\varepsilon}$. We have investigated this theoretical estimation numerically, and we have confirmed that for values of driving frequency such that $\tilde{\varepsilon}$ is large the corresponding frequency in the emission spectrum is large too, at a value around $\tilde{\varepsilon}\omega$.

By exploring Eq. (19), we find that the most important contribution of the second term of Eq. (20) is $-\tilde{\mu}\tilde{\varepsilon} \sin[\tilde{\varepsilon} J_0(\tilde{\Omega})\tau] \Sigma_{n=1}^{\infty} \frac{J_{2n}(\tilde{\Omega})\sin(2n\tau)}{2n}$. This term is responsible for the splitting of the even harmonics of the spectrum with splitting equal to $2\omega_{\mathrm{LF}}$. This splitting has been reported in two-level systems[22–26] and is also observed in our system once we describe it by means of the equivalent two-level system [see Fig. 1(a)]. In addition, we observe that for certain values of the Rabi frequency in the two-level system the odd harmonics (which are due to higher-order terms with respect to $\tilde{\varepsilon}$) are absent. However, the numerical solution of the time-dependent Schrödinger equation that describes the three-level two-electron QD system, predicts a more complex emission spectrum [see Fig. 1(b)]. Actually, we find peaks at all harmonics (even and odd) and at all places between the harmonics (from 0.5ω to $6.5\hbar\omega$), which cannot easily be explained by the analytic expression [see various harmonic terms in Eq. (19)].

In Fig. 2 we explore the two-electron QD molecule driven by an external electric field with frequency the same as in the previous case (Fig. 1) but with intensity such that the Rabi frequency of the field is $\hbar\Omega = 1.92386$ meV. In this case $\tilde{\Omega}$

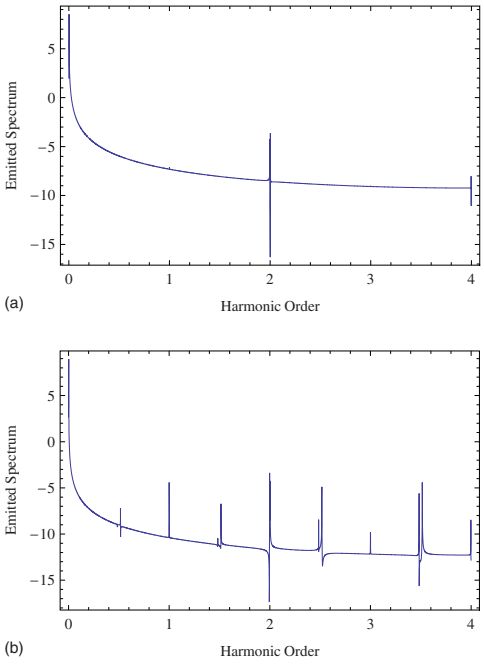

FIG. 1. (Color online) The numerically estimated emission spectrum of (a) the two-level system described by Eq. (10) and (b) the three-level two-electron QD molecule described by Eq. (6), for field parameters set at $\hbar\omega = \hbar\Omega = 1.6$ meV. The spectrum has been obtained after 128 cycles of the field. With harmonic order we mean that the emitted frequency is expressed in units of the external frequency.

$=2.4048255$, i.e., it is equal to the value of the first root of the zero-order Bessel function and the low frequency becomes zero [as $\omega_{\mathrm{LF}} = \tilde{\varepsilon} J_0(\tilde{\Omega})\omega$]. From the analytic expressions, we expect that there is no splitting of the harmonics of

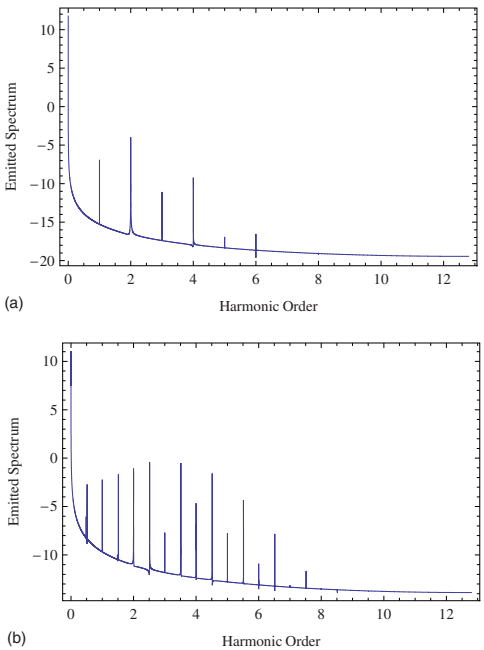

FIG. 2. (Color online) As in Fig. 1 but for external parameters set at $\hbar\omega = 1.6$ meV and $\hbar\Omega = 1.92386$ meV.

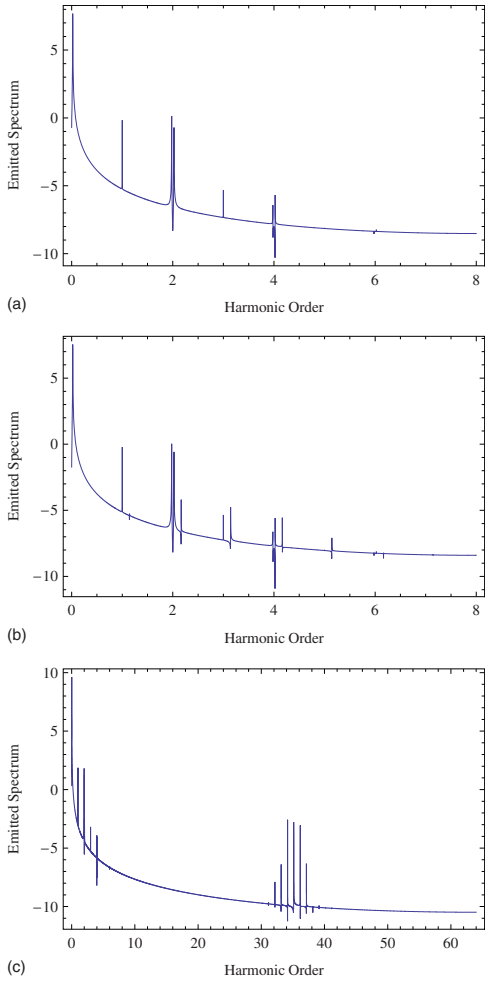

FIG. 3. (Color online) The low-harmonics part of the emission spectrum, numerically estimated for (a) the two-level system described by Eq. (10) and (b) the three-level two-electron QD molecule described by Eq. (6), for field parameters set at $\hbar\omega=\hbar\Omega=0.16$ meV. (c) The complete spectrum of case (b). The spectrum has been obtained after 128 cycles of the field.

the emission spectrum. This is actually observed once we treat our system as an equivalent two-level system [see Fig. 2(a)]. However, the numerical solution of the three-level two-electron QD system, predicts a more complex emission spectrum [see Fig. 2(b)]. As in Fig. 1 we find peaks at all harmonics (even and odd) and at most places between the harmonics.

By systematic investigation we set the limits of the two-level model. We have found that in this high-frequency driving-field regime, the lower the driving frequency the better the agreement between the two-level approximation and the numerical solution of the three-level system. For example in Figs. 3(a) and 3(b), we depict a case where the two-level approach and the numerical solution of the three-level system are in quite satisfactory agreement in the low-harmonics regime. As we have mentioned the lower the driving frequency the better the agreement, which depends on the strength of the applied field (Rabi frequency). Moreover, we have found that as the driving frequency becomes very low the dependence on the Rabi frequency practically disappears.

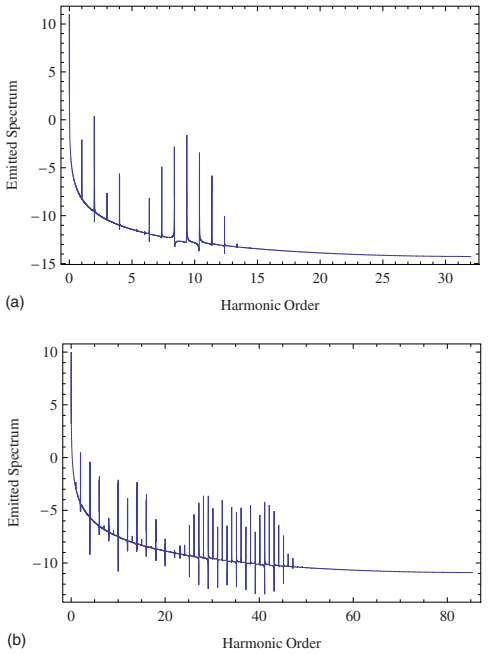

FIG. 4. (Color online) The numerically estimated emission spectrum of the two-electron QD molecule with external parameters set at (a) $\hbar\omega=\hbar\Omega=0.6$ meV and (b) $\hbar\omega=0.16$ meV and $\hbar\Omega=8\hbar\omega=1.28$ meV. The spectrum has been obtained after 128 cycles of the field.

In the case of very low driving-field frequency, a case studied in our previous work (Ref. 21) where high-harmonic generation is predicted, the agreement between the two- and the three-level model is very good.

From the same figure (Fig. 3), we clearly see that the agreement between the numerical predictions of the emission spectrum and the predictions of the two-level equivalent system is not good in the high-harmonic region, as the three-level system shows a region of high harmonics [Fig. 3(c)] not present in the two-level system.

We also investigate more systematically the high harmonics that appear in the emission spectrum [Fig. 3(c)]. We find that these well-separated regions of harmonics start to appear once the driving-field frequency is bellow 1 meV. Moreover, we see that the separation is such that the actual frequency of the center of the high-harmonic region takes always almost the same value. For example, compare Figs. 3(c) and 4(a). The position of the center of the high-harmonic part of the spectrum is for the case with driving frequency $\hbar\omega=0.16$ meV at the 35th harmonic [Fig. 3(c)] and for the case with driving frequency $\hbar\omega=0.6$ meV at the 9th harmonic [Fig. 4(a)]. The actual frequency is almost the same, in both cases around 5.5 meV. This is the case for even lower-driving field frequencies. It worth pointing out that this value is practically identical with the W-parameter [see Hamiltonian of the three-level system, Eq. (4)]. This behavior of the two-electron QD quantum system is not predicted by the simplified two-level model. Finally, we have shown that the emission spectrum in this region of high driving-field frequencies depends strongly on the intensity of the external electric field. Hence, for high value of the Rabi frequency the emission spectrum becomes different from the one reported in

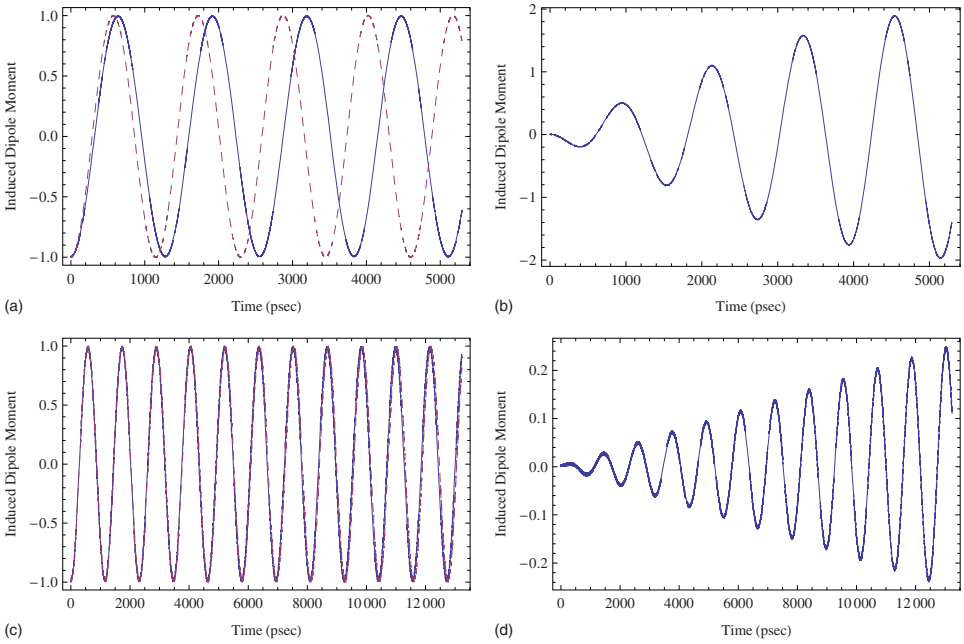

FIG. 5. (Color online) The numerically estimated normalized induced dipole moment $[\mu(t)/\tilde{\mu}]$ of the two-level system described by Eq. (10) and the three-level two-electron QD molecule described by Eq. (6). In plots (a) and (c) we depict both the two- (dotted curve) and three- (solid curve) level dipole moments. In plots (b) and (d) we depict the difference between the two- and the three-level dipole moments. The field parameters set at $\hbar\omega=\hbar\Omega=1.6$ meV for (a) and (b) and $\hbar\omega=\hbar\Omega=0.16$ meV for (c) and (d).

Figs. 3(c) and 4(a), with harmonics appearing in a very wide range [compare Figs. 3(c) and 4(b)].

Then, we try to understand the origin of these important findings in the emission spectra and find out some explanation for the discrepancies between the three-level and the simplified two-level models. As all spectra are derived from the induced dipole moments [Eq. (7)], we investigate and compare the time-dependent induced dipole moments. In Fig. 5 we plot the normalized dipole moments $[\mu(t)/\tilde{\mu}]$ for the cases studied in Figs. 1 and 3. For the case of Fig. 1 ($\hbar\omega=\hbar\Omega=1.6$ meV) we clearly see that the difference in the spectrum is purely related to the significant difference in the induced dipole moments [see Figs. 5(a) and 5(b)]. For the case studied in Fig. 3 ($\hbar\omega=\hbar\Omega=0.16$ meV) the two- and three-level dipole moments seem to be very similar with a minor phase difference [see Fig. 5(c)]. Actually this is not true as we can see from Fig. 5(d). There is a difference between the two dipole moments, which increases in magnitude with the time.

A very important feature of the three-level system, that never appears in the simplified two-level model, is the existence of harmonics at half-integer frequencies [i.e., at 0.5ω, 1.5ω, etc., see Fig. 3(b)]. We have investigated carefully these findings and have concluded that the existence of these harmonics depends on two factors, the driving-field frequency and the Rabi frequency. For example, if we get the spectrum for a case very similar to the one depicted in Fig. 3 but now with $\hbar\omega=0.15$ meV and for the same Rabi frequency, then we do not get peaks at half-integer frequencies but obtain peaks at positions much closer to the integer frequencies (not shown here). This reveals that the splitting of the harmonics depends strongly on the driving frequency. Moreover, as it is expected, we have found that the strength of the peaks depends on the Rabi frequency and for low driving-field intensity some features are almost absent. On the contrary, in the two-level model the terms of Eq. (20) never predict splitting of the order of half driving frequency no matter what is the value of the driving frequency and the Rabi frequency.

Before closing this discussion, we want to point out that as the driving frequency becomes lower we reach the regime we have investigated in our previous article (Ref. 21). In this case still Eqs. (19) and (20) are valid but the approximations we have followed in order to get solutions are not correct in this regime (specifically it is not proper to consider a perturbation theory with respect to parameter $\tilde{\varepsilon}$). But as it was found in Ref. 21 in this case the agreement between the three- and two-level system is very satisfactory. The reason is that in that case the two-level approach is based on a different theoretical model which relies on a level-crossing model.

IV. SUMMARY

In summary, in the present work we have calculated the emission spectrum of a GaAs two-electron QD molecule mainly in the region of high-frequency driving field. We have shown that the emission spectrum of the two-electron QD molecule driven by an external oscillatory electric field is rather complex. Very few of its features (harmonic peaks) can be explained by describing the system as an equivalent two-level system or by means of analytical expression derived in the context of the two-level system. Actually, the predictions of the analytic model are in quite good agreement with the results of the numerical calculations only for the low-frequency region of the emission spectrum. Moreover,

the analytic expressions predict the major peaks of the emission spectrum but they cannot account properly for the splitting of the harmonics. Finally, the analytic and the numerical two-level model do not predict any high-harmonics part in the emission spectrum for the high-frequency driving case.

ACKNOWLEDGMENTS

This work is supported by the K. Karatheodoris Project No. B.699 of the Research Committee of the University of Patras.

[1] G. Platero and R. Aguado, Phys. Rep. **395**, 1 (2004).
[2] P. I. Tamborenea and H. Metiu, Phys. Rev. Lett. **83**, 3912 (1999).
[3] P. Zhang and X.-G. Zhao, Phys. Lett. A **271**, 419 (2000).
[4] P. I. Tamborenea and H. Metiu, EPL **53**, 776 (2001).
[5] P. Zhang and X.-G. Zhao, J. Phys.: Condens. Matter **13**, 8389 (2001).
[6] C. E. Creffield and G. Platero, Phys. Rev. B **65**, 113304 (2002).
[7] P. Zhang, Q.-K. Xue, X.-G. Zhao, and X. C. Xie, Phys. Rev. A **66**, 022117 (2002).
[8] L. M. Wang, S. Q. Duan, X. G. Zhao, C. S. Liu, and B. K. Ma, Chin. Phys. Lett. **20**, 1340 (2003).
[9] E. Paspalakis, Phys. Rev. B **67**, 233306 (2003).
[10] Y. S. Liu and H. Chen, Phys. Lett. A **328**, 400 (2004).
[11] E. Paspalakis and A. F. Terzis, J. Appl. Phys. **95**, 1603 (2004).
[12] Z. Jiang, D. Suqing, and X.-G. Zhao, Phys. Lett. A **330**, 260 (2004).
[13] Z. Jiang, S.-Q. Duan, and X.-G. Zhao, Phys. Lett. A **340**, 309 (2005).
[14] C. Lin and X. L. Zhang, Commun. Theor. Phys. **45**, 357 (2006).
[15] U. Hohenester, J. Fabian, and F. Troiani, Opt. Commun. **264**, 426 (2006).
[16] A. F. Terzis, S. G. Kosionis, and E. Paspalakis, J. Phys. B **40**, S331 (2007).
[17] H. E. Tureci, J. M. Taylor, and A. Imamoglu, Phys. Rev. B **75**, 235313 (2007).
[18] G. E. Murgida, D. A. Wisniacki, and P. I. Tamborenea, Phys. Rev. Lett. **99**, 036806 (2007).
[19] R. Nepstad, L. Sælen, and J. P. Hansen, Phys. Rev. B **77**, 125315 (2008).
[20] L. Sælen, R. Nepstad, I. Degani, and J. P. Hansen, Phys. Rev. Lett. **100**, 046805 (2008).
[21] A. F. Terzis and E. Paspalakis, J. Appl. Phys. **97**, 023523 (2005).
[22] Y. Dakhnovskii and H. Metiu, Phys. Rev. A **48**, 2342 (1993).
[23] R. Bavli and H. Metiu, Phys. Rev. A **47**, 3299 (1993).
[24] Y. Dakhnovskii and R. Bavli, Phys. Rev. B **48**, 11020 (1993).
[25] H. Wang, V.-N. Freire, and X.-G. Zhao, Phys. Rev. A **58**, 1531 (1998).
[26] V. Delgado and J. M. G. Llorente, J. Phys. B **33**, 5403 (2000).
[27] F. I. Gauthey, C. H. Keitel, P. L. Knight, and A. Maquet, Phys. Rev. A **52**, 525 (1995).
[28] F. I. Gauthey, B. M. Garraway, and P. L. Knight, Phys. Rev. A **56**, 3093 (1997).
[29] P. P. Corso, L. Lo Cascio, and F. Persico, Phys. Rev. A **58**, 1549 (1998).
[30] C. Figueira de Morisson Faria, M. Dorr, and W. Sandner, Phys. Rev. A **58**, 2990 (1998).
[31] E. Fiordilino, Phys. Rev. A **59**, 876 (1999).
[32] C. F. de Morisson Faria and I. Rotter, Phys. Rev. A **66**, 013402 (2002).
[33] C.-P. Liu, S.-Q. Gong, R.-X. Li, and Z.-Z. Xu, Phys. Rev. A **69**, 023406 (2004).
[34] G. Orlando, P. P. Corso, and E. Fiordilino, Phys. Rev. A **72**, 013408 (2005).
[35] W.-F. Yang, S.-Q. Gong, R.-X. Li, S.-Q. Jin, and Z.-Z. Xu, Phys. Lett. A **362**, 37 (2007).
[36] M. Abramowitz and I. A. Stegun, *Handbook of Mathematical Functions with Formulas, Graphs and Mathematical Tables* (Dover, New York, 1965), Chap. 9, p. 361.